EURASIAN PHYSICAL TECHNICAL JOURNAL

2025, Volume 22, No.4 (54)

https://doi.org/10.31489/2025N4/123-131

Received: 25/06/2025 Revised: 28/11/2025 Accepted: 22/12/2025 Published online: 29/12/2025

Original Research Article

UDC 537.533,535.31

COLLIMATOR AND TELESCOPIC MODES OF A CATHODE LENS

Trubitsyn A.A.*, Grachev E.Yu., Kochergin E.G., Serezhin A.A.

Ryazan State Radio Engineering University named after V.F. Utkin, Ryazan, Russia
Corresponding author: assur@bk.ru

Abstract. *One way to improve the performance of emission systems (electron microscopes, microfocus X-ray tubes, etc.) is to reduce cathode lens aberrations. Such a reduction is only possible through a thorough theoretical analysis of their electron-optical schemes. This research attempts to develop tools for modeling a cathode lens with a virtually arbitrary electrode configuration in the paraxial approximation, and the conditions for implementing the collimator and telescopic modes have been determined. The relationship between the parameters that provide the specified operating modes of the lens has been studied. Electron-optical schemes have been developed that guarantee collimator and telescopic modes of a cathode lens of a real (non-idealized) design.*

Keywords: electron optics, electrostatic lens, paraxial optics, potential distribution.

1. Introduction

A cathode lens (immersion objective, electron gun) is used for the primary formation and acceleration of the electron flow in charged particles sources of emission systems [1-3], such as electron spectrometers, electron microscopes, microfocus X-ray tubes, electron lithographs, etc. The diameter of the probe (focal spot) of the emission system depends on the quality of the device's output optics, while the magnitude of the generated probe current is determined by the source brightness [4]. Source brightness is the most important parameter [5]. To approach the theoretically limiting (Langmuir) brightness [6, 7], reducing the aberrations of the cathode lens is primarily necessary. However, despite numerous studies on the numerical modeling of electron guns [8-10] and quantitative improvement of their parameters, the cathode lens, even in the paraxial approximation, remains virtually unstudied. This is primarily due to the overestimation of the capabilities of numerical experiments by modern researchers. This paper attempts to develop and advance tools for studying the paraxial properties of a cathode lens and apply these tools to lenses with arbitrary electrode geometries.

A cathode lens is characterized by the fact that the cathode is immersed in an electric field created by potentials on the anode and the focusing electrode. The paper considers low-current lenses, i.e. those whose perveance does not exceed 10^{-2} μA/V$^{3/2}$ [11].

Numerical analysis of a low-current cathode lens, when the space charge can be neglected during calculating the field and single trajectories of charged particles, does not cause any problems. However, the capabilities of numerical analysis are limited by the enumeration of various design options, and therefore the only advantage of numerical experimentation in creating new devices is the reduction in the cost of development. Discovering a new quality of the designed device is possible only by means of theoretical analysis. Theoretical optics includes paraxial optics and the theory of aberrations.

2. Theoretical technique

The fundamental equation of paraxial electron optics is a second-order linear differential equation, which in the cylindrical coordinate system *r*0*z* for axially symmetric systems has the form [12]

$$r'' + \frac{\Phi'}{2\Phi} r' + \frac{\Phi''}{4\Phi} r = 0. \tag{1}$$

The general solution of equation (1) for a known potential distribution $\Phi=\Phi(z)$ on the axis of symmetry will be the particle trajectory $r=r(z)$. In the case of common types of electron lenses, such as immersion, Einzel, and aperture lenses, this equation is solved by standard numerical methods. When modeling a cathode lens, difficulties arise in calculating the trajectories of electrons in the region where they start from the cathode. In the paraxial approximation (1), these difficulties are due to a mathematical singularity in the potential distribution function on the surface $z=z_c$ of the cathode C, since $\Phi_c=\Phi(z_c)=0$, and $\Phi'_c\neq 0$. From here on in the article, we will use the subscript "c" for the values of all functions on the cathode surface. Fortunately, a sufficiently developed theory [13] for solving second-order equations with this type of singularity allows us to find both particular solutions, where one of the particular solutions of equation (1), $p=p(z)$, is an analytic function, and the second solution, $g=g(z)$, has the following expression in terms of analytic function

$$g = \sqrt{\Phi} q, \tag{2}$$

where $q=q(z)$ is an analytical function, which, as follows from (1) and (2), satisfies the equation

$$q'' + \frac{3}{2}\frac{\Phi'}{\Phi} q' + \frac{3}{4}\frac{\Phi''}{\Phi} q = 0. \tag{3}$$

It can be shown that the functions $p(z)$ and $q(z)$ satisfy the same boundary conditions

$$p_c = q_c = 1, \qquad p'_c = q'_c = -\frac{\Phi''_c}{2\Phi'_c}, \tag{4}$$

and the particular solutions $p(z)$ and $g(z)$ are related to each other by the relation

$$\sqrt{\Phi}(pg' - gp') = \frac{1}{2}\Phi'_c, z > z_c$$

Partial solutions are key functions in paraxial optics and allow us to calculate electron trajectories, determine magnification, cardinal elements, and more. The general solution, which is the trajectory equation in our case, can be expressed as a linear combination of linearly independent partial solutions

$$r(z) = ap(z) + bg(z),$$

where the constants *a* and *b* are determined from the initial conditions on the cathode surface. In the uniquely significant work [14], expressions for *a* and *b* for a cathode lens were obtained and the equation for the paraxial trajectory was written

$$r(z) = r_c \cdot p(z) + \frac{2\sqrt{\varepsilon}}{\Phi'_c} \sin\vartheta_c \cdot g(z), \tag{5}$$

where ε is the energy of an electron emitted from the cathode and it is a mathematical quantity of the second order of smallness, r_c is the radius of the electron's start from the surface of the cathode, ϑ_c is the initial angle of movement relative to the axis of symmetry.

In the following calculations, the expression for the first derivative $r'(z)$ will be used, which is found by differentiating equation (5):

$$r'(z) = r_c \cdot p'(z) + \frac{2\sqrt{\varepsilon}}{\Phi'_c} \sin\vartheta_c \cdot g'(z). \quad (6)$$

To date, cathode lenses have been little studied, even in the paraxial approximation, especially since elements of the theory of aberrations of this lens [14] are awaiting their time. Almost all the available results of studying the paraxial cathode lens are presented in [15], using the approximation of infinitely small interelectrode gaps. In this approximation, the axial distribution of the potential $\Phi(z)$ was obtained using the method of separation of variables.

3. Numerical experiment

The main drawback of the variable separation method is that it can only describe potential distribution functions in idealized electron-optical systems (EOS) with simple electrode configurations. Our theoretical approach, presented in this paper, allows us to study a wide range of cathode lenses with virtually arbitrary boundaries. To analyze the paraxial properties and calculate the aberrations of real (non-idealized) cathode lenses, the software FOCUS CL [16] has been developed and is being promoted.

The software FOCUS CL contains 1) a graphical editor for inputting the cathode lens design, 2) a block for calculating the axial potential distribution using the boundary element method and visualizing it, 3) a block for calculating particular solutions $p(z)$, $g(z)$ using the Runge-Kutta method and constructing trajectories $r(z)$. The boundary element method is used to solve the external Dirichlet problem, where each electrode is represented by a closed contour with a given potential on it. It should be noted that obtaining the integral equation relating the potentials of the simple and double layers [17] is based on the second Green's formula. The integral equation in this formulation provides the possibility of solving the field problem for systems with electrodes of arbitrary thickness and shape, having corners and kinks. The axial potential distribution function $\Phi(z)$ is defined in a set of discrete nodes. The software has a built-in option for smoothing the nodal values $\Phi(z)$ using the sliding polynomial method [18]. The derivatives $\Phi'(z)$, $\Phi''(z)$, $p'(z)$ and $g'(z)$ are calculated using six-node numerical differentiation formulas [19].

It should be noted that well-known methods such as the finite difference method (FDM) and the finite element method (FEM) are not very suitable for calculating the axial potential distribution. These methods require calculating the field over the entire analyzed region and only then extracting the axial distribution. This means that the time required to solve the problem using these methods is orders of magnitude higher than using the BEM. Therefore, using the FDM and FEM for solving cathode lens synthesis problems is impractical. Note that the unique modes of the cathode lens [15] can be detected by analyzing equations (5) and (6). The collimator mode, characterized by the transformation of the flow emitted by a point source (r_c=0) into a parallel flow $r'(z)$=0 at the exit of the lens in image space at $z \geq z_{im}$, as can be seen from (6), is determined by the system

$$\begin{cases} r_c = 0, \\ g'(z) = 0, z \geq z_{im}, \end{cases} \quad (7)$$

whereas the telescopic mode, which causes the transformation of the parallel flow ($\sin\vartheta_c = 0$) of electrons emitted from a flat cathode into a parallel $r'(z)$=0 at the exit from the lens at $z \geq z_{im}$, will be fixed by the system of expressions

$$\begin{cases} \sin\vartheta_c = 0, \\ p'(z) = 0, z \geq z_{im}, \end{cases} \quad (8)$$

The left boundary z_{im} of the image space coincides with the boundary of the region of the uniform field, which is located at a distance from the center of the lens approximately equal to the inner diameter d of the cylindrical electrodes. Searching for the parameters at which the lens switches to the collimator or telescopic mode by checking the second condition of (7) and (8) is convenient because the form of particular solutions $g(z)$ and $p(z)$ does not depend on the initial values of the electron energy ε and the angle ϑ_c, but is determined only by fixed boundary conditions (4), which in turn are associated with the distribution $\Phi(z)$ of a particular EOS. Of practical interest are three-electrode cathode lenses (Fig. 1), consisting of a grounded cathode C, in the simplest case disk-shaped, and control and accelerating cylindrical electrodes with potentials V and V_{acc}, respectively. Given the same diameter d of the cylindrical electrodes and a significant excess of length over

.

the diameter of the accelerating electrode, the specific form of $\Phi(z)$ will be determined by the length l and the potential V of the control electrode.

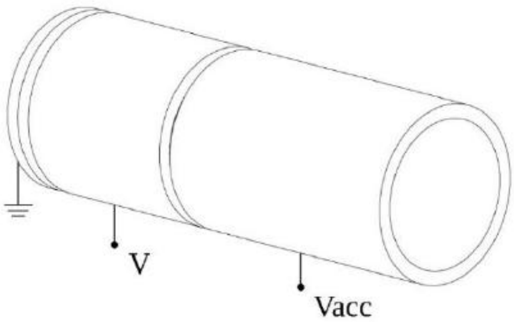

Fig.1. A three-electrode cathode lens consisting of a grounded cathode, a control electrode with potential V, and an accelerating electrode with potential V_{acc}

This article, firstly, tests the proposed methodology for studying a three-electrode cathode lens with a numerically determined axial potential distribution in the two specific modes mentioned above—collimator and telescope ones. Secondly, it presents lens designs with actual interelectrode gap sizes and defines the criteria for both lens modes. Presenting the criteria of the two modes in one article allows for their comparative evaluation. Since the results of the lens study in telescope mode have been previously published [20] and are publicly available, this mode for a real lens design is considered in less detail.

3.1 Collimator mode of the three-electrode cathode lens

Fig. 2, a demonstrates the collimator mode of a three-electrode cathode lens. Electrons are emitted by a point source in the range of initial angles ϑ_c = -70° to +70° with a step of 10°. The relative initial energy of the particles is $\varepsilon/V_{acc} = 10^{-3}$, the relative length of the control electrode is $l/d = 1$, and its relative potential is V/V_{acc} = 0.49. The selected range of angles ϑ_c = -70° to +70° allows us to exclude uninformative "tails" in the angular distributions of electrons, which appear in calculations near the boundaries of the full range of angles -90° and +90°. An additional argument in favor of choosing a slightly reduced range of initial angles ϑ_c in calculations is the cosine distribution of electrons by angles during emission from a solid, which sharply reduces the number of particles emitted by the cathode just near ±90°.

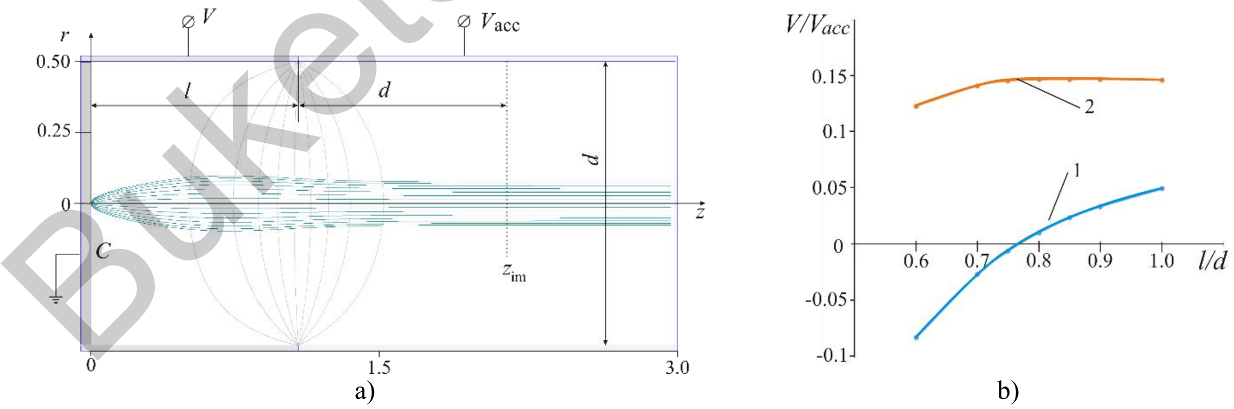

Fig. 2. Results of modeling a paraxial three-electrode cathode lens: a – results of trajectory analysis in graphical form, b – graph of the relationship between the potential of the intermediate electrode V and its length l: 1 - in the collimator mode, 2 – in the telescopic mode.

Based on the calculation results, it was concluded that for each length l of the control electrode, varied in the range acceptable in practice, the potential V of this electrode is found, which ensures the collimator mode (7); moreover, it is noteworthy that the graph of the relative dependence $V/V_{acc}=f(l/d)$ (Fig. 2, b) crosses zero, i.e. the potential V can have both positive and negative values. Note that negative values of the potential are less preferable in practice, since in this case a bipolar source of electric power for the cathode lens would be required. The graphical dependence in Fig. 2, b is calculated for the case of a small value of the insulating interelectrode gaps δ=0.002d. In the work [15], as already noted, a lens with infinitely small insulating gaps was studied. A comparison of the results of both studies shows their practical coincidence, since the relative difference in the obtained values does not exceed $\Delta V/V_{acc}$ = 0.2%, which directly confirms the impeccability of the conclusions of works [14, 15] and the correctness of the numerical-analytical technique for studying paraxial cathode lenses presented here, implemented in the FOCUS CL application [16]. At the same time, the high accuracy of the calculation results of the proposed paraxial technique is demonstrated by comparison with the "reference" trajectory numerical analysis [21] of a cathode lens.

In this case, the electric field is numerically determined over the entire working region of the lens, not just on the axis, and the electron trajectories are the result of numerical integration over time of the classical Newtonian equations of motion. Such a comparison made it possible to identify a tendency for some natural growth of the calculation error in the paraxial approximation with an increase in the initial angle ϑ_c up to 70 ° and, most importantly, to fix the upper limit of this error $\Delta r/d$ = 0.1 %. Here $\Delta r=|r_{parax}(z_{im})-r_{num}(z_{im})|$ is the absolute deviation of the trajectories calculated using the paraxial $r_{parax}(z)$ and numerical $r_{num}(z)$ methods [21] in the $z=z_{im}$ plane. The error level, which is small beyond expectations and equal to 0.1% at large angles ϑ_c, emphasizes not only the high reliability of the results of the paraxial trajectories calculating in accordance with expression (5), but also the applicability of the paraxial method proposed in this paper for the trajectory analysis of wide-acceptance EOSs, and under low time-consuming conditions.

3.2 Telescopic mode of a three-electrode cathode lens

The graphs of particular solutions $p(z)$ and $g(z)$ for a three-electrode cathode lens with parameters l/d = 0.7 and V/V_{acc} = 0.141 (see Fig. 3, a) are shown in Fig. 3, b. On the $p(z)$ dependence, one can distinguish the section $p(z)$=const at $z \geq z_{im}$, where $z_{im} \approx l+d$, which is a specific feature of the telescopic mode. The proposed approach to analyzing particular solutions made it possible to establish a relationship between the length l and the potential V of the control electrode (Fig. 2, b) in the telescopic mode (8).

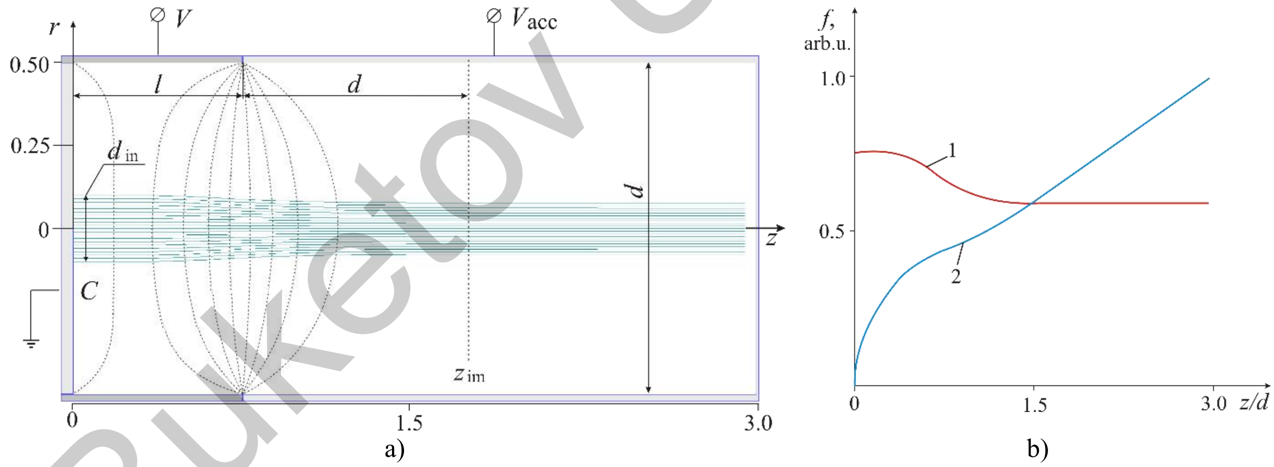

Fig.3. Results of modeling of a paraxial three-electrode cathode lens:
a – electrons trajectories (5) with ϑ_c=0 and r_c = 0÷0.5d_{in} in the telescopic mode, d_{in} = 0.2d is an initial flow diameter,
b – particular solutions: 1 – $p(z)$, 2 – $g(z)$.

A detailed numerical study of the cathode lens of the design under consideration in the telescopic mode is presented in the author's work [20].

3.3 Cathode lenses of a real (non-idealized) design

The proposed numerical method for studying paraxial cathode lenses with numerical determination of the potential distribution on the axis of symmetry makes it possible to synthesize lenses those designs are not idealized, but are as close as possible to real ones, in particular leneses insulating interelectrode gaps are capable of maintaining electrical strength at voltages of 10 - 100 kV and higher.

4. Results and Discussion

The scheme of a lens with interelectrode gaps, the size of which does not allow electrical breakdowns to develop, is shown in Fig. 4, a. The synthesis of a lens to ensure the collimator mode (7) consisted in finding the potential V of the intermediate electrode for its predetermined length l. Calculations have shown that the lens scheme (Fig. 4) also has the property of changing the sign of the electrode potential in the process of successive change of its length, while the zero potential of the intermediate electrode V/V_{acc} = 0 fixes the collimator mode for the electrode of length $l = 0.7041d$. Fig. 5 shows the axial distribution of the potential $\Phi(z)$ in this lens included in equations (1) and (3) and its two derivatives, as well as a graph of the particular solution $g(z)$ with the section $g(z)$=const characteristic of the collimator mode at $z \geq z_{im}$.

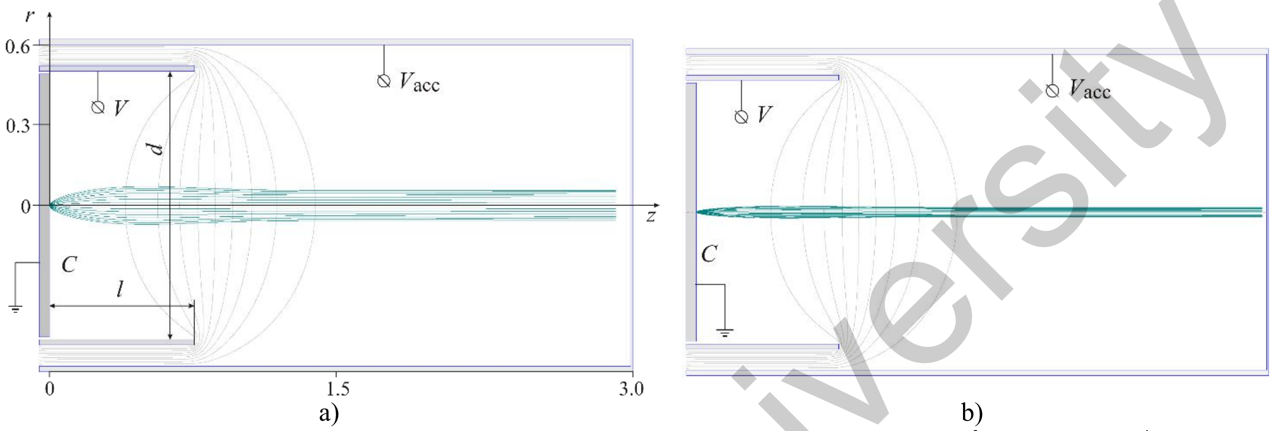

Fig. 4. Results of numerical analysis of a real design cathode lens: a - $\varepsilon/V_{acc}= 10^{-3}$, b - $\varepsilon/V_{acc}= 10^{-4}$.

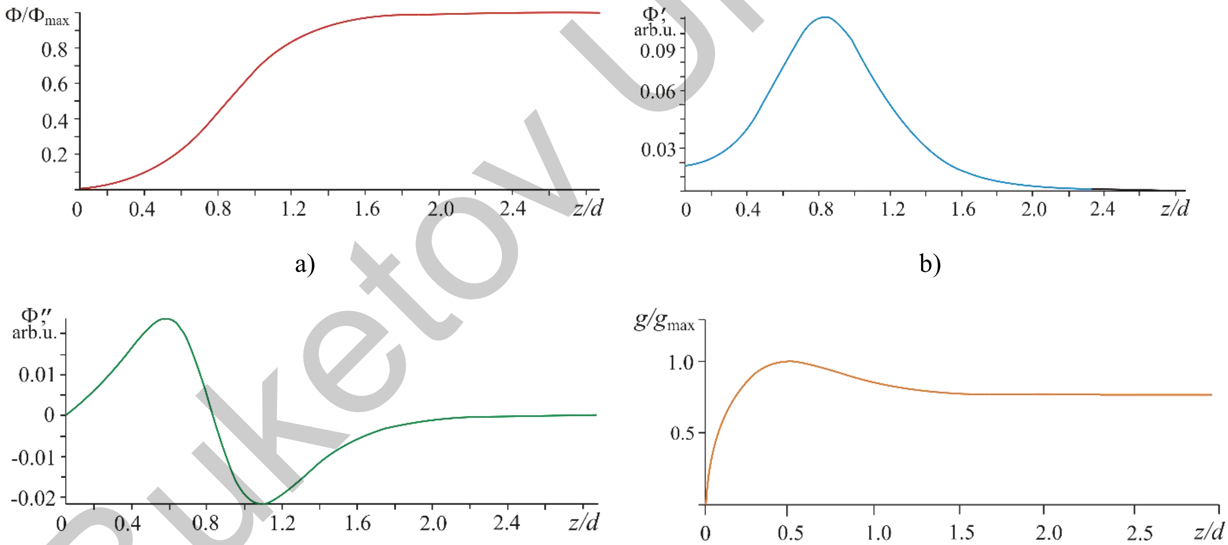

Fig. 5. Axial potential distribution (a) in a lens of the real design, the first (b) and second (c) derivatives of the distribution, and a graph of the particular solution g(z) (d). The subscript "max" indicates the maximum value of the function

Note that Fig. 4, a demonstrates the results of the numerical (not in the paraxial approximation) trajectory analysis of the lens in the range of angles ϑ_c=-70° - +70° with the initial relative energy of electrons $\varepsilon/V_{acc}= 10^3$. The average absolute deviation of the trajectory inclination angle from 0° in the $z=z_{im}$ plane is approximately equal to $\overline{|\vartheta_c(z_{im})|} = 0.09°$, and the numerically determined position of the second-order focus [22] relative to the central angle ϑ_c=0 is $z_f \approx -100d$, which allows us to speak about a high degree of parallelism of the electron trajectories with the z axis in the field-free space $z \geq z_{im}$. With increasing accelerating voltage (the ratio ε/V_{acc} decreases), a natural narrowing of the electron beam is observed (Fig. 4, b) with an improvement in the degree of parallelism: $\overline{|\vartheta_c(z_{im})|} = 0.007°$, $z_f \approx -400d$ for $\varepsilon/V_{acc} = 10^{-4}$.

The collimator mode can play a positive role in the development of emission systems with pointed cathodes - field emission and Schottky cathodes - since the parallel electron flow occupies a minimum volume of phase space in a series of converging and diverging flows and therefore can be focused into a spot of minimum diameter. To determine the telescopic mode conditions in a lens of a real design, we use the same algorithm. By varying the potential V of a control electrode of a specific length l, we check the fulfillment of the second condition of the system of expressions (8). The axial potential distribution $\Phi(z)$ for each value of V is calculated using the boundary element method. As a specific example of a lens of a real design in telescopic mode (Fig. 6), we present the following parameters: $l/d = 0.7$, $V = 0.137V_{acc}$.

After the telescopic mode conditions have been detected, a trajectory analysis is carried out with a real spread of initial angles in order to study the properties of the real lens design in more depth. Figure 6 shows the graphical results of a numerical trajectory analysis of a lens with a real design. The analysis used a range of initial angles of ϑ_c = -70° to +70° at an electron emission energy of $\varepsilon = 10^{-6}\ V_{acc}$. The initial flow diameter was chosen to be $d_{in} = 0.2d$.

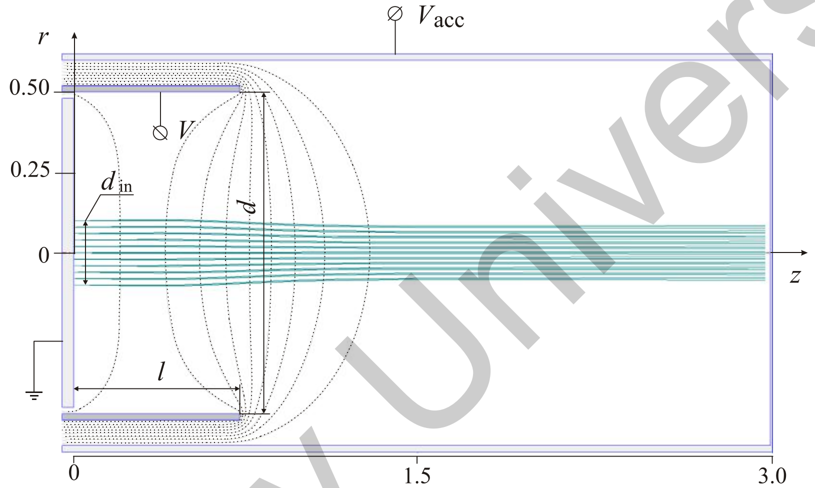

Fig. 6. Results of numerical analysis of a real design cathode lens in telescopic mode: $\varepsilon/V_{acc} = 10^{-6}$, $d_{in}/d = 0.2$, $r_c = -0.5d_{in} \div 0{,}5d_{in}$, $\vartheta_c = -70° \div +70°$.

The trajectory analysis results suggest that a high level of flow parallelism is maintained at the system exit. Quantitative estimates of the flow characteristics in the exit plane $z = l + 2d$ are as follows:

- the inclination angle of the central trajectories with $\vartheta_c = 0$ increases with increasing starting radius r_c, but does not exceed 0.02° at $r_c = d_{in}/2$;

- the spread of the angles of the two outer trajectories with $\vartheta_c = \pm 70°$ does not exceed ±0.08° for the entire initial range of r_c.

The telescopic mode will prove productive in the creation of emission systems with large-diameter flat cathodes, such as photocathodes.

5. Conclusion

This article develops an approach to theoretical analysis of a cathode lens in the paraxial approximation by calculating the potential distribution on the lens axis using the numerical boundary element method. BEM is the optimal method for solving this problem in terms of computation speed and accuracy, enabling both analysis and the synthesis of cathode lenses with specific properties in real time. The effectiveness of a two-stage development of cathode lens designs is demonstrated. After discovering new lens modes using theoretical paraxial optics, its electron-optical parameters are refined and studied using more accurate numerical methods.

This work includes the development of software for studying cathode lenses of a real (non-idealized) design in the paraxial approximation; criteria for the collimator and telescope modes of a three-electrode cathode lens with small and realistic interelectrode gaps are determined.

The development of methods for theoretical analysis of cathode lenses will enable targeted solutions to increase the brightness of accelerated electron sources.

Conflict of interest statement
The authors declare that they have no conflict of interest in relation to this research, whether financial, personal, authorship or otherwise, that could affect the research and its results presented in this paper.

CRediT author statement
Trubitsyn A.: Conceptualization, Methodology, Supervision; **Grachev E.**: Investigation, Formal Analysis, Writing-Reviewing and Editing; **Kochergin E.**: Software and Analysis, Validation; **Serezhin A.**: Writing - original draft, Review and Editing. The final manuscript was read and approved by all authors.

Funding
The research was funded by the Russian Science Foundation (grant no. 25-29-00124).

References

1 Guo X. (2024) *The Schottky emitter as a source for multi-electron-beam instruments*. Dissertation (TU Delft), Delft University of Technology. doi.org/10.4233/uuid:304cdd73-083a-4f89-ad47- f192e84a5313

2 Ohsawa S., Ikeda M., Sugimura T., Tawada M., Hozumi Y. and Kanno K. (2005) *High Brightness Electron Gun for X-Ray Source*. Proceedings of the 2005 Particle Accelerator Conference, Knoxville, TN, USA. 1488-1490. doi: 10.1109/PAC.2005.1590809.

3 Hideo Morishita, Takashi Ohshima, Kazuo Otsuga, Makoto Kuwahara, Toshihide Agemura, Yoichi Ose (2021) Brightness evaluation of pulsed electron gun using negative electron affinity photocathode developed for time-resolved measurement using scanning electron microscope. *Ultramicroscopy*, 230, 113386. doi.org/10.1016/j.ultramic.2021.113386.

4 Bronsgeest M. S., Barth J. E., Swanson L. W., Kruit P. (2008) Probe current, probe size, and the practical brightness for probe forming systems. *Journal of Vacuum Science & Technology B*. 26 (3), 949-955. doi: 10.1116/1.2907780

5 Han C, Sul I, Cho B. (2017) Edge shadow projection method for measuring the brightness of electron guns. *Rev Sci Instrum,* 88(2), 023302. doi: 10.1063/1.4974956.

6 Lauer R. (2020*) Characteristics of triode electron guns.* In P. W. Hawkes (Ed.), *Advances in imaging and electron physics*, 215. 195–266. Academic Press, London. doi.org/10.1016/bs.aiep.2020.06.007.

7 Kuriki M. (2022) *Theoretical limit of electron beam brightness generated from electron guns*. Proceedings of the 19th Annual Meeting of Particle Accelerator Society of Japan, October 18 – 21, Kyushu University, 1065-1069.

8 Fujita S, Shimoyama H. (2005) A new evaluation method of electron optical performance of high beam current probe forming systems. *J Electron Microsc (Tokyo)*. 54(5), 413-427. doi: 10.1093/jmicro/dfi063.

9 Cardona J. D., DietrichIsh k., Mukul M. et al. (2022) Simulations of a new electron gun for the TITAN EBIT. Journal of Physics: Conference Series 2244, 012075. doi:10.1088/1742-6596/2244/1/012075.

10 Wang RC., Jiao JQ., Zang K. et al. (2025) Development of pulsed electron gun based on PIC simulation. *Radiat Detect Technol Methods*. https://doi.org/10.1007/s41605-025-00591-z.

11 Sushkov A.D. (2022) *Vacuum Electronics. Physical and Technical Foundations*. Lan, St. Petersburg. 464. [in Russian]. Available at: https://lanbook.com/catalog/inzhenerno-tekhnicheskie-nauki/vakuumnaya-elektronika-fiziko-tehnicheskie-osnovy-3883606/?utm_source

12 Hawkes P.W. (1972) *Electron Optics and Electron Microscopy*. Taylor & Francis Ltd., London, 244. https://doi.org/10.1002/crat.19720071212

13 Smirnov V.I. (1974) *Course of Higher Mathematics, Vol. 3, Part 2*. Nauka, Moscow, 672. [in Russian] Available at: https://www.litres.ru/book/vladimir-smirnov-3/kurs-vysshey-matematiki-tom-iii-chast-2-6988781/?utm_source

14 Yakushev E.M. (2013) *Theory and Computation of Electron Mirrors: The Central Particle Method.* In P. W. Hawkes (Ed.), *Advances in imaging and electron physics*, 178. 147–247. Academic Press, London. https://doi.org/10.1016/B978-0-12-407701-0.00003-0

15 Yakushev E.M., Bimurzaev S.B., & Kholodov M.A. (2016) To Determine the Cardinal Elements and Angular Characteristics of Cathode Lenses with Rotational Symmetry. *Bulletin of the Aktobe Regional State University named after K. Zhubanov*, 44(2), 32 – 40. [in Russian] Available at: https://vestnik.arsu.kz/ index.php/hab/issue/view/12/18

16 Trubitsyn A.A., Grachev E.Yu., &Kochergin E.G. (2024) *Focus CL Program for Modeling Cathode Lenses. Certificate of State Registration of Computer Program No. 2024680471*. [in Russian]

17 Brebbia C.A., Telles J.C.F., Wroubel L.C. (2012) *Boundary Element Techniques: Theory and Applications in Engineering*. Springer Berlin Heidelberg, 464. https://doi.org/10.1007/978-3-642-48860-3

18 Korn G.A., Korn T.M. (2013) *Mathematical Handbook for Scientists and Engineers.* Dover Publications Inc, NY. 1152. Available at: https://www.scribd.com/document/530807645/Mathematics-Handbook-for-Scientists-and-Engineers?utm_source=chatgpt.com

19 Abramovits M., Stigan I.A. (1965) *Handbook of Special Functions with Formulas, Graphs, and Mathematical Tables*. Dover Publications Inc, NY. 1046. Available at: https://personal.math.ubc.ca/~cbm/aands/abramowitz_and_stegun.pdf

20 Trubitsyn A.A., Grachev E.Yu., & Kochergin E.G. (2025) Telescopic Mode of a Cathode Lens. *Pis'ma v zhurnal tekhnicheskoy fiziki, 51 (13), 32 – 36. [in Russian].* https://doi.org/10.61011/PJTF.2025.13.60701.20284 [in Russian]

21 Gurov V.S., Saulebekov A.O., & Trubitsyn A.A. (2015) *Analytical, Approximate-Analytical and Numerical Methods in the Design of Energy Analyzers.* In P. W. Hawkes (Ed.), Advances in Imaging and Electron Physics, 192. Academic Press, London, 212. https://doi.org/10.1016/S1076-5670(15)00103-2

22 Trubitsyn A.A. (2001) A Correlation Method of Search for Higher-Order Angular Focusing. *Technical Physics*, 46 (5), 630-631. https://doi.org/10.1134/1.1372960

AUTHORS' INFORMATION

Trubitsyn, Andrey Afanasievich – Doctor of Physical and Mathematical Sciences, Professor, Department of Industrial Electronics, Ryazan State Radio Engineering University, Russia; ORCID iD 0000-0002-9337-8947; assur@bk.ru

Grachev, Evgeny Yuryevich – Candidate of Engineering Sciences, Associated Professor, Department of Industrial Electronics, Ryazan State Radio Engineering University, Russia; ORCID iD 0000-0001-7813-7769; monopol_rus@mail.ru

Kochergin, Eduard Gennadievich – graduate student, Department of Industrial Electronics, Ryazan State Radio Engineering University, Russia; ORCID iD 0009-0007-7436-2708; a kochergin_aduard@mail.ru

Serezhin, Andrey Alexandrovich – Candidate of Engineering Sciences, Associated Professor, Department of Industrial Electronics, Ryazan State Radio Engineering University, Russia; ORCID iD 0000-0001-8134-8970; a andrei-serezhin@yandex.ru

.